

Measurement of y_{CP} in $D^0 - \bar{D}^0$ oscillation using quantum correlations in
 $e^+e^- \rightarrow D^0\bar{D}^0$ at $\sqrt{s} = 3.773$ GeV

M. Ablikim¹, M. N. Achasov^{8,a}, X. C. Ai¹, O. Albayrak⁴, M. Albrecht³, D. J. Ambrose⁴³, A. Amoroso^{47A,47C},
 F. F. An¹, Q. An⁴⁴, J. Z. Bai¹, R. Baldini Ferroli^{19A}, Y. Ban³⁰, D. W. Bennett¹⁸, J. V. Bennett⁴, M. Bertani^{19A},
 D. Bettoni^{20A}, J. M. Bian⁴², F. Bianchi^{47A,47C}, E. Boger^{22,h}, O. Bondarenko²⁴, I. Boyko²², R. A. Briere⁴, H. Cai⁴⁹,
 X. Cai¹, O. Cakir^{39A,b}, A. Calcaterra^{19A}, G. F. Cao¹, S. A. Cetin^{39B}, J. F. Chang¹, G. Chelkov^{22,c}, G. Chen¹,
 H. S. Chen¹, H. Y. Chen², J. C. Chen¹, M. L. Chen¹, S. J. Chen²⁸, X. Chen¹, X. R. Chen²⁵, Y. B. Chen¹,
 H. P. Cheng¹⁶, X. K. Chu³⁰, G. Cibinetto^{20A}, D. Cronin-Hennessy⁴², H. L. Dai¹, J. P. Dai³³, A. Dbeysi¹³,
 D. Dedovich²², Z. Y. Deng¹, A. Denig²¹, I. Denysenko²², M. Destefanis^{47A,47C}, F. De Mori^{47A,47C}, Y. Ding²⁶,
 C. Dong²⁹, J. Dong¹, L. Y. Dong¹, M. Y. Dong¹, S. X. Du⁵¹, P. F. Duan¹, J. Z. Fan³⁸, J. Fang¹, S. S. Fang¹,
 X. Fang⁴⁴, Y. Fang¹, L. Fava^{47B,47C}, F. Feldbauer²¹, G. Felici^{19A}, C. Q. Feng⁴⁴, E. Fioravanti^{20A}, M. Fritsch^{13,21},
 C. D. Fu¹, Q. Gao¹, Y. Gao³⁸, Z. Gao⁴⁴, I. Garzia^{20A}, K. Goetzen⁹, W. X. Gong¹, W. Gradl²¹, M. Greco^{47A,47C},
 M. H. Gu¹, Y. T. Gu¹¹, Y. H. Guan¹, A. Q. Guo¹, L. B. Guo²⁷, T. Guo²⁷, Y. Guo¹, Y. P. Guo²¹, Z. Haddadi²⁴,
 A. Hafner²¹, S. Han⁴⁹, Y. L. Han¹, F. A. Harris⁴¹, K. L. He¹, Z. Y. He²⁹, T. Held³, Y. K. Heng¹, Z. L. Hou¹,
 C. Hu²⁷, H. M. Hu¹, J. F. Hu^{47A}, T. Hu¹, Y. Hu¹, G. M. Huang⁵, G. S. Huang⁴⁴, H. P. Huang⁴⁹, J. S. Huang¹⁴,
 X. T. Huang³², Y. Huang²⁸, T. Hussain⁴⁶, Q. Ji¹, Q. P. Ji²⁹, X. B. Ji¹, X. L. Ji¹, L. L. Jiang¹, L. W. Jiang⁴⁹,
 X. S. Jiang¹, J. B. Jiao³², Z. Jiao¹⁶, D. P. Jin¹, S. Jin¹, T. Johansson⁴⁸, A. Julin⁴², N. Kalantar-Nayestanaki²⁴,
 X. L. Kang¹, X. S. Kang²⁹, M. Kavatsyuk²⁴, B. C. Ke⁴, R. Kliemt¹³, B. Kloss²¹, O. B. Kolcu^{39B,d}, B. Kopf³,
 M. Kornicer⁴¹, W. Kuehn²³, A. Kupsc⁴⁸, W. Lai¹, J. S. Lange²³, M. Lara¹⁸, P. Larin¹³, C. H. Li¹, Cheng Li⁴⁴,
 D. M. Li⁵¹, F. Li¹, G. Li¹, H. B. Li¹, J. C. Li¹, Jin Li³¹, K. Li³², K. Li¹², P. R. Li⁴⁰, T. Li³², W. D. Li¹, W. G. Li¹,
 X. L. Li³², X. M. Li¹¹, X. N. Li¹, X. Q. Li²⁹, Z. B. Li³⁷, H. Liang⁴⁴, Y. F. Liang³⁵, Y. T. Liang²³, G. R. Liao¹⁰,
 D. X. Lin¹³, B. J. Liu¹, C. X. Liu¹, F. H. Liu³⁴, Fang Liu¹, Feng Liu⁵, H. B. Liu¹¹, H. H. Liu¹, H. H. Liu¹⁵,
 H. M. Liu¹, J. Liu¹, J. P. Liu⁴⁹, J. Y. Liu¹, K. Liu³⁸, K. Y. Liu²⁶, L. D. Liu³⁰, P. L. Liu¹, Q. Liu⁴⁰, S. B. Liu⁴⁴,
 X. Liu²⁵, X. X. Liu⁴⁰, Y. B. Liu²⁹, Z. A. Liu¹, Zhiqiang Liu¹, Zhiqing Liu²¹, H. Loehner²⁴, X. C. Lou^{1,e},
 H. J. Lu¹⁶, J. G. Lu¹, R. Q. Lu¹⁷, Y. Lu¹, Y. P. Lu¹, C. L. Luo²⁷, M. X. Luo⁵⁰, T. Luo⁴¹, X. L. Luo¹, M. Lv¹,
 X. R. Lyu⁴⁰, F. C. Ma²⁶, H. L. Ma¹, L. L. Ma³², Q. M. Ma¹, S. Ma¹, T. Ma¹, X. N. Ma²⁹, X. Y. Ma¹,
 F. E. Maas¹³, M. Maggiora^{47A,47C}, Q. A. Malik⁴⁶, Y. J. Mao³⁰, Z. P. Mao¹, S. Marcello^{47A,47C},
 J. G. Messchendorp²⁴, J. Min¹, T. J. Min¹, R. E. Mitchell^{19A}, X. H. Mo¹, Y. J. Mo⁵, C. Morales Morales¹³,
 K. Moriya¹⁸, N. Yu. Muchnoi^{8,a}, H. Muramatsu⁴², Y. Nefedov²², F. Nerling¹³, I. B. Nikolaev^{8,a}, Z. Ning¹,
 S. Nisar⁷, S. L. Niu¹, X. Y. Niu¹, S. L. Olsen³¹, Q. Ouyang¹, S. Pacetti^{19B}, P. Patteri^{19A}, M. Pelizaeus³,
 H. P. Peng⁴⁴, K. Peters⁹, J. L. Ping²⁷, R. G. Ping¹, R. Poling⁴², Y. N. Pu¹⁷, M. Qi²⁸, S. Qian¹, C. F. Qiao⁴⁰,
 L. Q. Qin³², N. Qin⁴⁹, X. S. Qin¹, Y. Qin³⁰, Z. H. Qin¹, J. F. Qiu¹, K. H. Rashid⁴⁶, C. F. Redmer²¹, H. L. Ren¹⁷,
 M. Ripka²¹, G. Rong¹, X. D. Ruan¹¹, V. Santoro^{20A}, A. Sarantsev^{22,f}, M. Savrié^{20B}, K. Schoenning⁴⁸,
 S. Schumann²¹, W. Shan³⁰, M. Shao⁴⁴, C. P. Shen², P. X. Shen²⁹, X. Y. Shen¹, H. Y. Sheng¹, M. R. Shepherd¹⁸,
 W. M. Song¹, X. Y. Song¹, S. Sosio^{47A,47C}, S. Spataro^{47A,47C}, B. Spruck²³, G. X. Sun¹, J. F. Sun¹⁴, S. S. Sun¹,
 Y. J. Sun⁴⁴, Y. Z. Sun¹, Z. J. Sun¹, Z. T. Sun¹⁸, C. J. Tang³⁵, X. Tang¹, I. Tapan^{39C}, E. H. Thorndike⁴³,
 M. Tiemens²⁴, D. Toth⁴², M. Ullrich²³, I. Uman^{39B}, G. S. Varner⁴¹, B. Wang²⁹, B. L. Wang⁴⁰, D. Wang³⁰,
 D. Y. Wang³⁰, K. Wang¹, L. L. Wang¹, L. S. Wang¹, M. Wang³², P. Wang¹, P. L. Wang¹, Q. J. Wang¹,
 S. G. Wang³⁰, W. Wang¹, X. F. Wang³⁸, Y. D. Wang^{19A}, Y. F. Wang¹, Y. Q. Wang²¹, Z. Wang¹, Z. G. Wang¹,
 Z. H. Wang⁴⁴, Z. Y. Wang¹, T. Weber²¹, D. H. Wei¹⁰, J. B. Wei³⁰, P. Weidenkaff²¹, S. P. Wen¹, U. Wiedner³,
 M. Wolke⁴⁸, L. H. Wu¹, Z. Wu¹, L. G. Xia³⁸, Y. Xia¹⁷, D. Xiao¹, Z. J. Xiao²⁷, Y. G. Xie¹, G. F. Xu¹, L. Xu¹,
 Q. J. Xu¹², Q. N. Xu⁴⁰, X. P. Xu³⁶, L. Yan⁴⁴, W. B. Yan⁴⁴, W. C. Yan⁴⁴, Y. H. Yan¹⁷, H. X. Yang¹, L. Yang⁴⁹,
 Y. Yang⁵, Y. X. Yang¹⁰, H. Ye¹, M. Ye¹, M. H. Ye⁶, J. H. Yin¹, B. X. Yu¹, C. X. Yu²⁹, H. W. Yu³⁰, J. S. Yu²⁵,
 C. Z. Yuan¹, W. L. Yuan²⁸, Y. Yuan¹, A. Yuncu^{39B,g}, A. A. Zafar⁴⁶, A. Zallo^{19A}, Y. Zeng¹⁷, B. X. Zhang¹,
 B. Y. Zhang¹, C. Zhang²⁸, C. C. Zhang¹, D. H. Zhang¹, H. H. Zhang³⁷, H. Y. Zhang¹, J. J. Zhang¹, J. L. Zhang¹,
 J. Q. Zhang¹, J. W. Zhang¹, J. Y. Zhang¹, J. Z. Zhang¹, K. Zhang¹, L. Zhang¹, S. H. Zhang¹, X. Y. Zhang³²,
 Y. Zhang¹, Y. H. Zhang¹, Y. T. Zhang⁴⁴, Z. H. Zhang⁵, Z. P. Zhang⁴⁴, Z. Y. Zhang⁴⁹, G. Zhao¹, J. W. Zhao¹,
 J. Y. Zhao¹, J. Z. Zhao¹, Lei Zhao⁴⁴, Ling Zhao¹, M. G. Zhao²⁹, Q. Zhao¹, Q. W. Zhao¹, S. J. Zhao⁵¹,
 T. C. Zhao¹, Y. B. Zhao¹, Z. G. Zhao⁴⁴, A. Zhemchugov^{22,h}, B. Zheng⁴⁵, J. P. Zheng¹, W. J. Zheng³²,
 Y. H. Zheng⁴⁰, B. Zhong²⁷, L. Zhou¹, Li Zhou²⁹, X. Zhou⁴⁹, X. K. Zhou⁴⁴, X. R. Zhou⁴⁴, X. Y. Zhou¹, K. Zhu¹,
 K. J. Zhu¹, S. Zhu¹, X. L. Zhu³⁸, Y. C. Zhu⁴⁴, Y. S. Zhu¹, Z. A. Zhu¹, J. Zhuang¹, B. S. Zou¹, J. H. Zou¹

(BESIII Collaboration)

- ¹ Institute of High Energy Physics, Beijing 100049, People's Republic of China
- ² Beihang University, Beijing 100191, People's Republic of China
- ³ Bochum Ruhr-University, D-44780 Bochum, Germany
- ⁴ Carnegie Mellon University, Pittsburgh, Pennsylvania 15213, USA
- ⁵ Central China Normal University, Wuhan 430079, People's Republic of China
- ⁶ China Center of Advanced Science and Technology, Beijing 100190, People's Republic of China
- ⁷ COMSATS Institute of Information Technology, Lahore, Defence Road, Off Raiwind Road, 54000 Lahore, Pakistan
- ⁸ G.I. Budker Institute of Nuclear Physics SB RAS (BINP), Novosibirsk 630090, Russia
- ⁹ GSI Helmholtzcentre for Heavy Ion Research GmbH, D-64291 Darmstadt, Germany
- ¹⁰ Guangxi Normal University, Guilin 541004, People's Republic of China
- ¹¹ GuangXi University, Nanning 530004, People's Republic of China
- ¹² Hangzhou Normal University, Hangzhou 310036, People's Republic of China
- ¹³ Helmholtz Institute Mainz, Johann-Joachim-Becher-Weg 45, D-55099 Mainz, Germany
- ¹⁴ Henan Normal University, Xinxiang 453007, People's Republic of China
- ¹⁵ Henan University of Science and Technology, Luoyang 471003, People's Republic of China
- ¹⁶ Huangshan College, Huangshan 245000, People's Republic of China
- ¹⁷ Hunan University, Changsha 410082, People's Republic of China
- ¹⁸ Indiana University, Bloomington, Indiana 47405, USA
- ¹⁹ (A)INFN Laboratori Nazionali di Frascati, I-00044, Frascati, Italy; (B)INFN and University of Perugia, I-06100, Perugia, Italy
- ²⁰ (A)INFN Sezione di Ferrara, I-44122, Ferrara, Italy; (B)University of Ferrara, I-44122, Ferrara, Italy
- ²¹ Johannes Gutenberg University of Mainz, Johann-Joachim-Becher-Weg 45, D-55099 Mainz, Germany
- ²² Joint Institute for Nuclear Research, 141980 Dubna, Moscow region, Russia
- ²³ Justus Liebig University Giessen, II. Physikalisches Institut, Heinrich-Buff-Ring 16, D-35392 Giessen, Germany
- ²⁴ KVI-CART, University of Groningen, NL-9747 AA Groningen, The Netherlands
- ²⁵ Lanzhou University, Lanzhou 730000, People's Republic of China
- ²⁶ Liaoning University, Shenyang 110036, People's Republic of China
- ²⁷ Nanjing Normal University, Nanjing 210023, People's Republic of China
- ²⁸ Nanjing University, Nanjing 210093, People's Republic of China
- ²⁹ Nankai University, Tianjin 300071, People's Republic of China
- ³⁰ Peking University, Beijing 100871, People's Republic of China
- ³¹ Seoul National University, Seoul, 151-747 Korea
- ³² Shandong University, Jinan 250100, People's Republic of China
- ³³ Shanghai Jiao Tong University, Shanghai 200240, People's Republic of China
- ³⁴ Shanxi University, Taiyuan 030006, People's Republic of China
- ³⁵ Sichuan University, Chengdu 610064, People's Republic of China
- ³⁶ Soochow University, Suzhou 215006, People's Republic of China
- ³⁷ Sun Yat-Sen University, Guangzhou 510275, People's Republic of China
- ³⁸ Tsinghua University, Beijing 100084, People's Republic of China
- ³⁹ (A)Istanbul Aydin University, 34295 Sefakoy, Istanbul, Turkey; (B)Dogus University, 34722 Istanbul, Turkey; (C)Uludag University, 16059 Bursa, Turkey
- ⁴⁰ University of Chinese Academy of Sciences, Beijing 100049, People's Republic of China
- ⁴¹ University of Hawaii, Honolulu, Hawaii 96822, USA
- ⁴² University of Minnesota, Minneapolis, Minnesota 55455, USA
- ⁴³ University of Rochester, Rochester, New York 14627, USA
- ⁴⁴ University of Science and Technology of China, Hefei 230026, People's Republic of China
- ⁴⁵ University of South China, Hengyang 421001, People's Republic of China
- ⁴⁶ University of the Punjab, Lahore-54590, Pakistan
- ⁴⁷ (A)University of Turin, I-10125, Turin, Italy; (B)University of Eastern Piedmont, I-15121, Alessandria, Italy; (C)INFN, I-10125, Turin, Italy
- ⁴⁸ Uppsala University, Box 516, SE-75120 Uppsala, Sweden
- ⁴⁹ Wuhan University, Wuhan 430072, People's Republic of China
- ⁵⁰ Zhejiang University, Hangzhou 310027, People's Republic of China
- ⁵¹ Zhengzhou University, Zhengzhou 450001, People's Republic of China
- ^a Also at the Novosibirsk State University, Novosibirsk, 630090, Russia

^b Also at Ankara University, 06100 Tandogan, Ankara, Turkey

^c Also at the Moscow Institute of Physics and Technology, Moscow 141700, Russia and at the Functional Electronics Laboratory, Tomsk State University, Tomsk, 634050, Russia

^d Currently at Istanbul Arel University, 34295 Istanbul, Turkey

^e Also at University of Texas at Dallas, Richardson, Texas 75083, USA

^f Also at the PNPI, Gatchina 188300, Russia

^g Also at Bogazici University, 34342 Istanbul, Turkey

^h Also at the Moscow Institute of Physics and Technology, Moscow 141700, Russia

Abstract

We report a measurement of the parameter y_{CP} in $D^0 - \bar{D}^0$ oscillations performed by taking advantage of quantum coherence between pairs of $D^0\bar{D}^0$ mesons produced in e^+e^- annihilations near threshold. In this work, doubly-tagged $D^0\bar{D}^0$ events, where one D decays to a CP eigenstate and the other D decays in a semileptonic mode, are reconstructed using a data sample of 2.92 fb^{-1} collected with the BESIII detector at the center-of-mass energy of $\sqrt{s} = 3.773\text{ GeV}$. We obtain $y_{CP} = (-2.0 \pm 1.3 \pm 0.7)\%$, where the first uncertainty is statistical and the second is systematic. This result is compatible with the current world average.

Keywords: BESIII, $D^0 - \bar{D}^0$ oscillation, y_{CP} , quantum correlation

1. Introduction

1.1. Charm oscillation

It is well known that oscillations between meson and antimeson, also called mixing, can occur when the flavor eigenstates differ from the physical mass eigenstates. These effects provide a mechanism whereby interference in the transition amplitudes of mesons and antimesons may occur. They may also allow for manifestation of CP violation (CPV) in the underlying dynamics [1, 2]. Oscillations in the $K^0 - \bar{K}^0$ [3], $B^0 - \bar{B}^0$ [4] and $B_s^0 - \bar{B}_s^0$ [5] systems are established; their oscillation rates are well-measured and consistent with predictions from the standard model (SM) [6]. After an accumulation of strong evidence from a variety of experiments [7, 8, 9], $D^0 - \bar{D}^0$ oscillations were recently firmly established by LHCb [10]. The results were soon confirmed by CDF [11] and Belle [12].

The oscillations are conventionally characterized by two dimensionless parameters $x = \Delta m/\Gamma$ and $y = \Delta\Gamma/2\Gamma$, where Δm and $\Delta\Gamma$ are the mass and width differences between the two mass eigenstates and Γ is the average decay width of those eigenstates. The mass eigenstates can be written as $|D_{1,2}\rangle = p|D^0\rangle \pm q|\bar{D}^0\rangle$, where p and q are complex parameters and $\phi = \arg(q/p)$ is a CP -violating phase. Using the phase convention $CP|D^0\rangle = +|\bar{D}^0\rangle$, the CP eigenstates of the D meson can be written as

$$|D_{CP+}\rangle \equiv \frac{|D^0\rangle + |\bar{D}^0\rangle}{\sqrt{2}}, \quad |D_{CP-}\rangle \equiv \frac{|D^0\rangle - |\bar{D}^0\rangle}{\sqrt{2}}. \quad (1)$$

The difference in the effective lifetime between D decays to CP eigenstates and flavor eigenstates can be parameterized by y_{CP} . In the absence of direct CPV , but allowing for small indirect CPV , we have [13]

$$y_{CP} = \frac{1}{2} \left[y \cos\phi \left(\left| \frac{q}{p} \right| + \left| \frac{p}{q} \right| \right) - x \sin\phi \left(\left| \frac{q}{p} \right| - \left| \frac{p}{q} \right| \right) \right]. \quad (2)$$

Table 1: D final states reconstructed in this analysis.

Type	Mode
$CP+$	$K^+K^-, \pi^+\pi^-, K_S^0\pi^0\pi^0$
$CP-$	$K_S^0\pi^0, K_S^0\omega, K_S^0\eta$
Semileptonic	$K^\mp e^\pm\nu, K^\mp\mu^\pm\nu$

In the absence of CPV , one has $|p/q| = 1$ and $\phi = 0$, leading to $y_{CP} = y$.

Although $D^0 - \overline{D}^0$ mixing from short-distance physics is suppressed by the CKM matrix [14, 15] and the GIM mechanism [16], sizeable charm mixing can arise from long-distance processes and new physics [1, 17]. Current experimental precision [18] is not sufficient to conclude whether physics beyond the SM is involved, and further constraints are needed. So far, the most precise determination of the size of the mixing has been obtained by measuring the time-dependent decay rate in the $D \rightarrow K^\pm\pi^\mp$ channel [10, 11, 12]. However, the resulting information on the mixing parameters x and y is highly correlated. It is important to access the mixing parameters x and y directly to provide complementary constraints.

In this analysis, we use a time-integrated method to extract y_{CP} , as proposed in the references [19, 20, 21, 22], which uses threshold $D^0\overline{D}^0$ pair production in $e^+e^- \rightarrow \gamma^* \rightarrow D^0\overline{D}^0$. In this process, the $D^0\overline{D}^0$ pair is in a state of definite $C = -1$, such that the two D mesons necessarily have opposite CP eigenvalues. The method utilizes the semileptonic decays of D meson and hence, avoids the complications from hadronic effects in D decays, thus provides a clean and unique way to probe the $D^0 - \overline{D}^0$ oscillation.

1.2. Formalism

In the semileptonic decays of neutral D mesons (denoted as $D \rightarrow l$)¹, the partial decay width is only sensitive to flavor content and does not depend on the CP eigenvalue of the parent D meson. However, the total decay width of the $D_{CP\pm}$ does depend on its CP eigenvalue: $\Gamma_{CP\pm} = \Gamma(1 \pm y_{CP})$. Thus, the semileptonic branching fraction of the CP eigenstates $D_{CP\pm}$ is $\mathcal{B}_{D_{CP\pm} \rightarrow l} \approx \mathcal{B}_{D \rightarrow l}(1 \mp y_{CP})$, and y_{CP} can be obtained as

$$y_{CP} \approx \frac{1}{4} \left(\frac{\mathcal{B}_{D_{CP-} \rightarrow l}}{\mathcal{B}_{D_{CP+} \rightarrow l}} - \frac{\mathcal{B}_{D_{CP+} \rightarrow l}}{\mathcal{B}_{D_{CP-} \rightarrow l}} \right). \quad (3)$$

At BESIII, quantum-correlated $D^0\overline{D}^0$ pairs produced at threshold allow us to measure $\mathcal{B}_{D_{CP\pm} \rightarrow l}$. Specifically, we begin with a fully reconstructed D candidate decaying into a CP eigenstate, the so-called Single Tag (ST). We have thus tagged the CP eigenvalue of the partner D meson. For a subset of the ST events, the so-called Double Tag (DT) events, this tagged partner D meson is also observed via one of the semileptonic decay channels. CP violation in D decays is known to be very small [18], and can be safely neglected. Therefore, $\mathcal{B}_{D_{CP\mp} \rightarrow l}$ can be obtained as

$$\mathcal{B}_{D_{CP\mp} \rightarrow l} = \frac{N_{CP\pm;l}}{N_{CP\pm}} \cdot \frac{\varepsilon_{CP\pm}}{\varepsilon_{CP\pm;l}}, \quad (4)$$

where $N_{CP\pm}$ ($N_{CP\pm;l}$) and $\varepsilon_{CP\pm}$ ($\varepsilon_{CP\pm;l}$) denote the signal yields and detection efficiencies of ST decays $D \rightarrow CP\pm$ (DT decays $D\overline{D} \rightarrow CP\pm;l$), respectively. For CP eigenstates, as listed in Table 1, we choose modes with unambiguous CP content and copious yields. The CP violation in K_S^0 decays is known to be very small, it is therefore neglected. The semileptonic modes used for the DT in this analysis are $K^\mp e^\pm\nu$ and $K^\mp\mu^\pm\nu$.

1.3. The BESIII detector and data sample

The analysis presented in this paper is based on a data sample with an integrated luminosity of 2.92 fb^{-1} [23] collected with the BESIII detector [24] at the center-of-mass energy of $\sqrt{s} = 3.773 \text{ GeV}$.

¹Charge-conjugate modes are implied.

The BESIII detector is a general-purpose solenoidal detector at the BEPCII [25] double storage rings. The detector has a geometrical acceptance of 93% of the full solid angle. We briefly describe the components of BESIII from the interaction point (IP) outwards. A small-cell main drift chamber (MDC), using a helium-based gas to measure momenta and specific ionizations of charged particles, is surrounded by a time-of-flight (TOF) system based on plastic scintillators that determines the flight times of charged particles. A CsI(Tl) electromagnetic calorimeter (EMC) detects electromagnetic showers. These components are all situated inside a superconducting solenoid magnet, that provides a 1.0 T magnetic field parallel to the beam direction. Finally, a multi-layer resistive plate counter system installed in the iron flux return yoke of the magnet is used to track muons. The momentum resolution for charged tracks in the MDC is 0.5% for a transverse momentum of 1 GeV/c. The energy resolution for showers in the EMC is 2.5% (5.0%) for 1 GeV photons in the barrel (end cap) region. More details on the features and capabilities of BESIII can be found elsewhere [24].

High-statistics Monte Carlo (MC) simulations are used to evaluate the detection efficiency and to understand backgrounds. The GEANT4-based [26] MC simulation program is designed to simulate interactions of particles in the spectrometer and the detector response. For the production of $\psi(3770)$, the KKMC [27] package is used; the beam energy spread and the effects of initial-state radiation (ISR) are included. The MC samples consist of the $D\bar{D}$ pairs with consideration of quantum coherence for all modes relevant to this analysis, non- $D\bar{D}$ decays of $\psi(3770)$, ISR production of low-mass ψ states, and QED and $q\bar{q}$ continuum processes. The effective luminosity of the MC samples is about 10 times that of the analyzed data. Known decays recorded by the Particle Data Group (PDG) [6] are generated with EVTGEN [28, 29] using PDG branching fractions, and the remaining unknown decays are generated with LUNDCHARM [30]. Final-state radiation (FSR) of charged tracks is taken into account with the PHOTOS package [31].

2. Event selection and data analysis

Each charged track is required to satisfy $|\cos\theta| < 0.93$, where θ is the polar angle with respect to the beam axis. Charged tracks other than K_S^0 daughters are required to be within 1 cm of the IP transverse to the beam line and within 10 cm of the IP along the beam axis. Particle identification for charged hadrons h ($h = \pi, K$) is accomplished by combining the measured energy loss (dE/dx) in the MDC and the flight time obtained from the TOF to form a likelihood $\mathcal{L}(h)$ for each hadron hypothesis. The K^\pm (π^\pm) candidates are required to satisfy $\mathcal{L}(K) > \mathcal{L}(\pi)$ ($\mathcal{L}(\pi) > \mathcal{L}(K)$).

The K_S^0 candidates are selected with a vertex-constrained fit from pairs of oppositely charged tracks, which are required to be within 20 cm of the IP along the beam direction; no constraint in the transverse plane is required. The two charged tracks are not subjected to the particle identification discussed above, and are assumed to be pions. We impose $0.487 \text{ GeV}/c^2 < M_{\pi^+\pi^-} < 0.511 \text{ GeV}/c^2$, that is within about 3 standard deviations of the observed K_S^0 mass, and the two tracks are constrained to originate from a common decay vertex by requiring the χ^2 of the vertex fit to be less than 100. The decay vertex is required to be separated from the IP with a significance greater than two standard deviations.

Reconstructed EMC showers that are separated from the extrapolated positions of any charged tracks by more than 10 standard deviations are taken as photon candidates. The energy deposited in nearby TOF counters is included to improve the reconstruction efficiency and energy resolution. Photon candidates must have a minimum energy of 25 MeV for barrel showers ($|\cos\theta| < 0.80$) and 50 MeV for end cap showers ($0.84 < |\cos\theta| < 0.92$). The showers in the gap between the barrel and the end cap regions are poorly reconstructed and thus excluded. The shower timing is required to be no later than 700 ns after the reconstructed event start time to suppress electronic noise and energy deposits unrelated to the event. The η and π^0 candidates are reconstructed from pairs of photons. Due to the poorer resolution in the EMC end cap regions, those candidates with both photons coming from EMC end caps are rejected. The invariant mass $M_{\gamma\gamma}$ is required to be $0.115 \text{ GeV}/c^2 < M_{\gamma\gamma} < 0.150 \text{ GeV}/c^2$ for π^0 and $0.505 \text{ GeV}/c^2 < M_{\gamma\gamma} < 0.570 \text{ GeV}/c^2$ for η candidates. The photon pair is kinematically constrained to the nominal mass of the π^0 or η [6] to improve the meson four-vector calculation.

The ω candidates are reconstructed through the decay $\omega \rightarrow \pi^+\pi^-\pi^0$. For all modes with ω candidates, sideband events in the $M_{\pi^+\pi^-\pi^0}$ spectrum are used to estimate peaking backgrounds from non- ω $D \rightarrow K_S^0\pi^+\pi^-\pi^0$ decays. We take the signal region as (0.7600, 0.8050) GeV/ c^2 and the sideband regions as

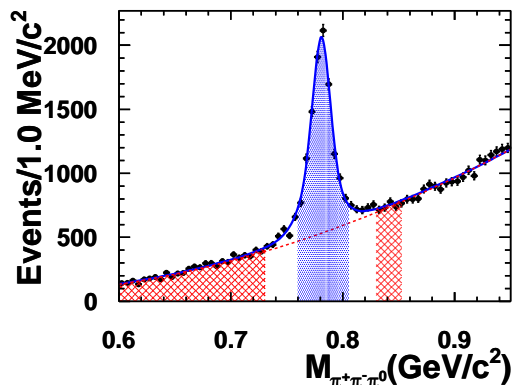


Figure 1: Fit to the invariant mass $M_{\pi^+\pi^-\pi^0}$ for events reconstructed from data. The solid line is the total fit and the dashed line shows the polynomial background. The shaded area shows the signal region and cross-hatched areas show the sidebands.

(0.6000, 0.7300) GeV/c^2 or (0.8300, 0.8525) GeV/c^2 . The upper edge of the right sideband is restricted because of the $K^*\rho$ background that alters the shape of $M_{\pi^+\pi^-\pi^0}$. The sidebands are scaled to the estimated peaking backgrounds in the signal region. The scaling factor is determined from a fit to the $M_{\pi^+\pi^-\pi^0}$ distribution in data, as shown in Fig. 1, where the ω signal is determined with the MC shape convoluted with a Gaussian whose parameters are left free in the fit to better match data resolution, and the background is modeled by a polynomial function.

2.1. Single tags using CP modes

To identify the reconstructed D candidates, we use two variables, the beam-constrained mass M_{BC} and the energy difference ΔE , which are defined as

$$M_{\text{BC}} \equiv \sqrt{E_{\text{beam}}^2/c^4 - |\vec{p}_D|^2/c^2}, \quad (5)$$

$$\Delta E \equiv E_D - E_{\text{beam}}, \quad (6)$$

where \vec{p}_D and E_D are the momentum and energy of the D candidate in the e^+e^- center-of-mass system, and E_{beam} is the beam energy. The D signal peaks at the nominal D mass in M_{BC} and at zero in ΔE . We accept only one candidate per mode per event; when multiple candidates are present, the one with the smallest $|\Delta E|$ is chosen. Since the correlation between ΔE and M_{BC} is found to be small, this will not bias the background distribution in M_{BC} . We apply the mode-dependent ΔE requirements listed in Table 2.

For K^+K^- and $\pi^+\pi^-$ ST modes, if candidate events contain only two charged tracks, the following requirements are applied to suppress backgrounds from cosmic rays and Bhabha events. First, we require at least one EMC shower separated from the tracks of the ST with energy larger than 50 MeV. Second, the two ST tracks must not be both identified as muons or electrons, and, if they have valid TOF times, the time difference must be less than 5 ns. Based on MC studies, no peaking background is present in M_{BC} in our ST modes except for the $K_S^0\pi^0$ mode. In the $K_S^0\pi^0$ ST mode, there are few background events from $D^0 \rightarrow \rho\pi$. From MC studies, the estimated fraction is less than 0.5%; this will be considered in the systematic uncertainties.

The M_{BC} distributions for the six ST modes are shown in Fig. 2. Unbinned maximum likelihood fits are performed to obtain the numbers of ST yields except in the $K_S^0\omega$ mode, for which a binned least-square fit is applied to the M_{BC} distribution after subtraction of the ω sidebands. In each fit, the signal shape is derived from simulated signal events convoluted with a bifurcated Gaussian with free parameters to account for imperfect modeling of the detector resolution and beam energy calibration. Backgrounds are described by the ARGUS [32] function. The measured ST yields in the signal region of $1.855 \text{ GeV}/c^2 < M_{\text{BC}} < 1.875 \text{ GeV}/c^2$ and the corresponding efficiencies are given in Table 3.

Table 2: Requirements on ΔE for ST D candidates.

Mode	Requirement (GeV)
K^+K^-	$-0.020 < \Delta E < 0.020$
$\pi^+\pi^-$	$-0.030 < \Delta E < 0.030$
$K_S^0\pi^0\pi^0$	$-0.080 < \Delta E < 0.045$
$K_S^0\pi^0$	$-0.070 < \Delta E < 0.040$
$K_S^0\omega$	$-0.050 < \Delta E < 0.030$
$K_S^0\eta$	$-0.040 < \Delta E < 0.040$

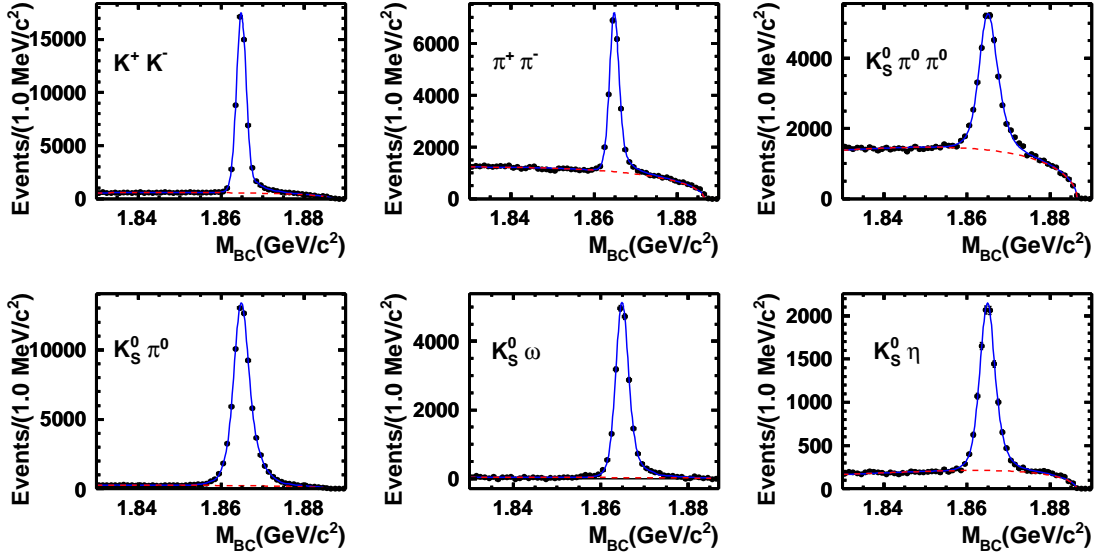


Figure 2: The M_{BC} distributions for ST D candidates from data. The solid line is the total fit and the dashed line shows the background contribution described by an ARGUS function.

Table 3: Yields and efficiencies of all ST and DT modes, where $N_{CP\pm}$ ($N_{CP\pm;l}$) and $\varepsilon_{CP\pm}$ ($\varepsilon_{CP\pm;l}$) denote signal yields and detection efficiencies of $D \rightarrow CP\pm$ ($D\bar{D} \rightarrow CP\pm;l$), respectively. The uncertainties are statistical only.

ST Mode	$N_{CP\pm}$	$\varepsilon_{CP\pm}$ (%)
K^+K^-	54494 ± 251	61.32 ± 0.18
$\pi^+\pi^-$	19921 ± 174	64.09 ± 0.18
$K_S^0\pi^0\pi^0$	24015 ± 236	16.13 ± 0.08
$K_S^0\pi^0$	71421 ± 285	40.67 ± 0.14
$K_S^0\omega$	20989 ± 243	13.44 ± 0.07
$K_S^0\eta$	9878 ± 117	34.39 ± 0.13
DT Mode	$N_{CP\pm;l}$	$\varepsilon_{CP\pm;l}$ (%)
$K^+K^-, Ke\nu$	1216 ± 40	39.80 ± 0.14
$\pi^+\pi^-, Ke\nu$	427 ± 23	41.75 ± 0.14
$K_S^0\pi^0\pi^0, Ke\nu$	560 ± 28	11.05 ± 0.07
$K_S^0\pi^0, Ke\nu$	1699 ± 47	26.70 ± 0.12
$K_S^0\omega, Ke\nu$	481 ± 30	9.27 ± 0.07
$K_S^0\eta, Ke\nu$	243 ± 17	22.96 ± 0.11
$K^+K^-, K\mu\nu$	1093 ± 37	36.89 ± 0.14
$\pi^+\pi^-, K\mu\nu$	400 ± 23	38.43 ± 0.15
$K_S^0\pi^0\pi^0, K\mu\nu$	558 ± 28	10.76 ± 0.08
$K_S^0\pi^0, K\mu\nu$	1475 ± 43	25.21 ± 0.12
$K_S^0\omega, K\mu\nu$	521 ± 27	8.75 ± 0.07
$K_S^0\eta, K\mu\nu$	241 ± 18	21.85 ± 0.11

2.2. Double tags of semileptonic modes

In each ST event, we search among the unused tracks and showers for semileptonic $D \rightarrow Ke(\mu)\nu$ candidates. We require that there be exactly two oppositely-charged tracks that satisfy the fiducial requirements described above.

In searching for $K\mu\nu$ decays, kaon candidates are required to satisfy $\mathcal{L}(K) > \mathcal{L}(\pi)$. If the two tracks can pass the criterion, the track with larger $\mathcal{L}(K)$ is taken as the K^\pm candidate, and the other track is assumed to be the μ candidate. The energy deposit in the EMC of the μ candidate is required to be less than 0.3 GeV. We further require the $K\mu$ invariant mass $M_{K\mu}$ to be less than 1.65 GeV/ c^2 to reject $D \rightarrow K\pi$ backgrounds. The total energy of remaining unmatched EMC showers, denoted as E_{extra} , is required to be less than 0.2 GeV to suppress $D \rightarrow K\pi\pi^0$ backgrounds. To reduce backgrounds from the $D \rightarrow Ke\nu$ process, the ratio $\mathcal{R}_{\mathcal{L}'}(e) \equiv \mathcal{L}'(e)/[\mathcal{L}'(e) + \mathcal{L}'(\mu) + \mathcal{L}'(\pi) + \mathcal{L}'(K)]$ is required to be less than 0.8, where the likelihood $\mathcal{L}'(i)$ for the hypothesis $i = e, \mu, \pi$ or K is formed by combining EMC information with the dE/dx and TOF information.

To select $Ke\nu$ events, electron candidates are required to satisfy $\mathcal{L}'(e) > 0.001$ and $\mathcal{R}'_{\mathcal{L}'}(e) > 0.8$, where $\mathcal{R}'_{\mathcal{L}'}(e) \equiv \mathcal{L}'(e)/[\mathcal{L}'(e) + \mathcal{L}'(\pi) + \mathcal{L}'(K)]$. If both tracks satisfy these requirements, the one with larger $\mathcal{R}'_{\mathcal{L}'}(e)$ is taken as the electron. The remaining track is required to satisfy $\mathcal{L}(K) > \mathcal{L}(\pi)$.

The variable U_{miss} is used to distinguish semileptonic signal events from background:

$$U_{\text{miss}} \equiv E_{\text{miss}} - c|\vec{p}_{\text{miss}}|, \quad (7)$$

where,

$$E_{\text{miss}} \equiv E_{\text{beam}} - E_K - E_l, \quad (8)$$

$$\vec{p}_{\text{miss}} \equiv - \left[\vec{p}_K + \vec{p}_l + \hat{p}_{\text{ST}} \sqrt{E_{\text{beam}}^2/c^2 - c^2 m_D^2} \right], \quad (9)$$

$E_{K(l)}$ ($\vec{p}_{K(l)}$) is the energy (three-momentum) of K^\mp (l^\pm), \hat{p}_{ST} is the unit vector in the direction of the reconstructed CP -tagged D and m_D is the nominal D mass. The use of the beam energy and the nominal D mass for the magnitude of the CP -tagged D improves the U_{miss} resolution. Since E equals to $|\vec{p}|c$ for a neutrino, the signal peaks at zero in U_{miss} .

The U_{miss} distributions are shown in Fig. 3, where the tagged- D is required to be in the region of $1.855 \text{ GeV}/c^2 < M_{\text{BC}} < 1.875 \text{ GeV}/c^2$. DT yields, obtained by fitting the U_{miss} spectra, are listed in Table 3. Unbinned maximum likelihood fits are performed for all modes except for modes including ω . For modes including an ω , binned least-square fits are performed to the ω sideband-subtracted U_{miss} distributions. In each fit, the $Ke\nu$ or $K\mu\nu$ signal is modeled by the MC-determined shape convoluted with a bifurcated Gaussian where all parameters are allowed to vary in the fit. Backgrounds for $Ke\nu$ are well described with a first-order polynomial. However, in the $K\mu\nu$ mode, backgrounds are more complex and consist of three parts. The primary background comes from $D \rightarrow K\pi\pi^0$ decay. To better control this background, we select a sample of $D \rightarrow K\pi\pi^0$ in data by requiring $E_{\text{extra}} > 0.5 \text{ GeV}$, in which the U_{miss} shape of $K\pi\pi^0$ is proved to be basically the same as that in the region of $E_{\text{extra}} < 0.2 \text{ GeV}$ in MC simulation. The selected $K\pi\pi^0$ sample is used to extract the resolution differences in the U_{miss} shape of $K\pi\pi^0$ in MC and data, and to obtain the $D \rightarrow K\pi\pi^0$ yields in $E_{\text{extra}} > 0.5 \text{ GeV}$ region. Then, in fits to U_{miss} , the $K\pi\pi^0$ is described by the resolution-corrected shape from MC simulations and its size is fixed according to the relative simulated efficiencies of the $E_{\text{extra}} > 0.5 \text{ GeV}$ and $E_{\text{extra}} < 0.2 \text{ GeV}$ selection criteria. The second background from $Ke\nu$ events is modeled by a MC-determined shape. Its ratio to the signal yields is about 3.5% based on MC studies and is fixed in the fits. Background in the third category includes all other background processes, which are well described with a first-order polynomial.

3. Systematic uncertainties

Most sources of uncertainties for the ST or DT efficiencies, such as tracking, PID, and π^0 , η , K_S^0 reconstruction, cancel out in determining y_{CP} . The main systematic uncertainties come from the background veto, modeling of the signals and backgrounds, fake tagged signals, and the CP -purity of ST events.

The cosmic and Bhabha veto is applied only for the KK and $\pi\pi$ ST events which have only two tracks. The effect of this veto is estimated based on MC simulation. We compare the cases with and without this requirement and the resultant relative changes in ST efficiencies are about 0.3% for both the KK and $\pi\pi$ modes. The resulting systematic uncertainty on y_{CP} is 0.001.

Peaking backgrounds are studied for different ST modes, especially for $\rho\pi$ backgrounds in the $K_S^0\pi^0$ tag mode and $K_S^0\pi^+\pi^-\pi^0$ backgrounds in the $K_S^0\omega$ tag mode. Based on a study of the inclusive MC samples, the fraction of peaking backgrounds in $K_S^0\pi^0$ is 0.3%. The uncertainties on y_{CP} caused by this is about 0.001. Uncertainties from the sideband subtraction of peaking backgrounds for the $K_S^0\omega$ mode are studied by changing the sideband and signal regions; changes in the efficiency-corrected yields are negligible.

Fits to the M_{BC} and U_{miss} spectra could induce systematic errors by the modeling of the signal and background shape. The MC-determined signal shapes convoluted with a Gaussian are found to describe the data well, and systematic uncertainties from the modeling of the signal are assumed to be negligible. To estimate uncertainties from modeling of backgrounds, different methods are considered. For the CP ST yields, we include an additional background component to account for the $\psi(3770) \rightarrow D\bar{D}$ process with a shape determined by MC simulation whose yield is determined in the fit. The uncertainties in the fits to M_{BC} are uncorrelated among different tag modes, and the obtained change on y_{CP} is 0.001. For the DT semileptonic yields, the polynomial functions that are used to describe backgrounds in our nominal fits are replaced by a shape derived from MC simulations. For the $K\mu\nu$ mode, the size of the main background $K\pi\pi^0$ is fixed in our nominal fit, so the statistical uncertainties of the number of selected $K\pi\pi^0$ events introduces a systematic error. To estimate the associated uncertainty, we vary its size by ± 1 standard deviation based on the selected $K\pi\pi^0$ samples. Systematic uncertainties due to the U_{miss} fits are treated as positively correlated among different tag modes. We take the maximum change on the resultant y_{CP} , that is 0.006, as systematic uncertainty.

The DT yields are obtained from the fit to the U_{miss} spectra. However, one also has to consider events that peak at U_{miss} but are backgrounds in the M_{BC} spectra, the so-called fake tagged signals. This issue is

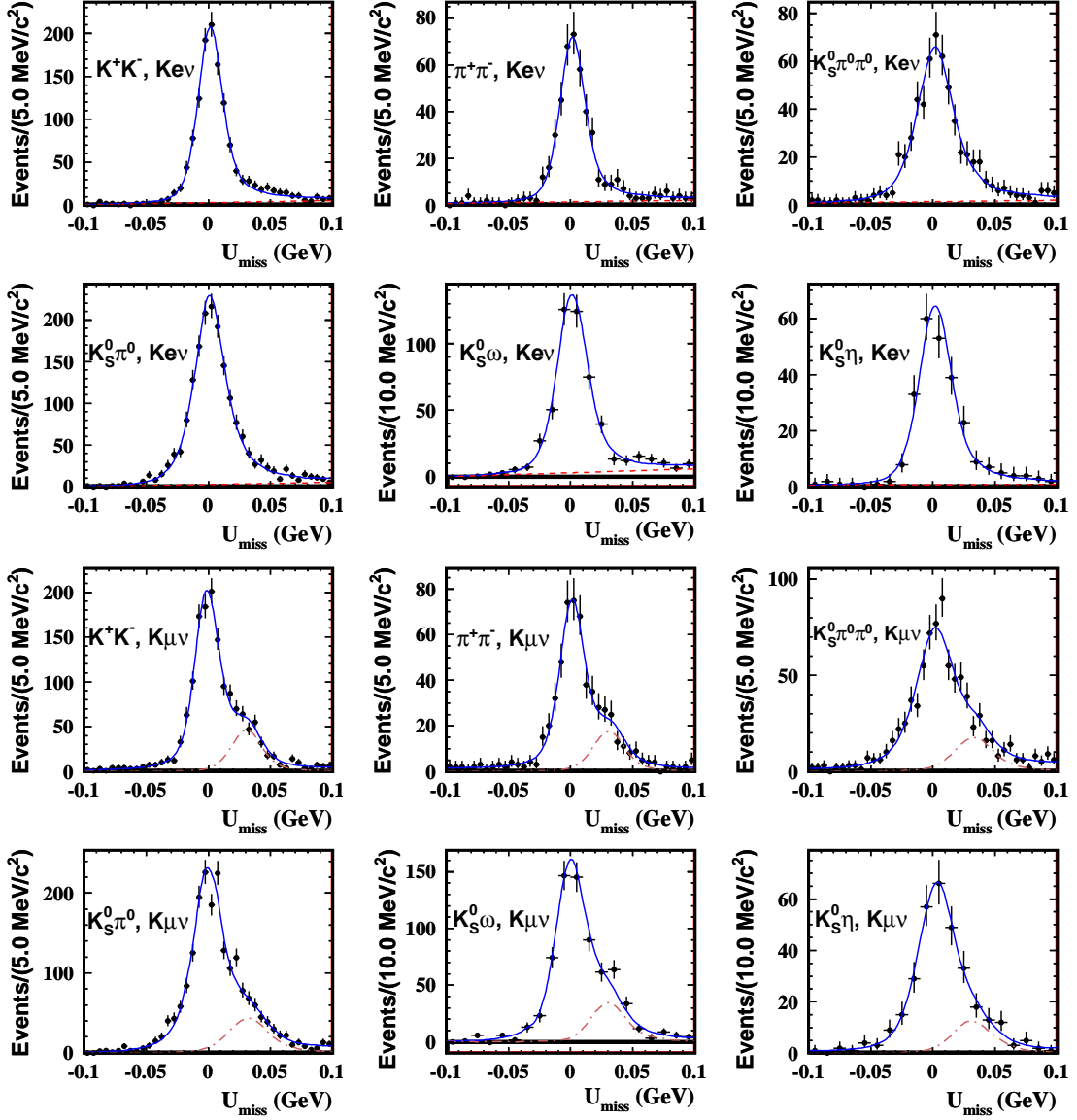


Figure 3: Fit to the U_{miss} distributions for selected DT events from data. In each plot, the solid line is the total fit, the dashed line in Kev shows the contribution of polynomial backgrounds, and the dash-dotted line in $K\mu\nu$ shows the contribution of the main $K\pi\pi^0$ backgrounds.

Table 4: Summary of systematic uncertainties. Relative systematic uncertainties are listed for each tag mode in percent, while the resulting absolute uncertainties on y_{CP} are shown in the last column. Negligible uncertainties are denoted by “-”.

	K^+K^-	$\pi^+\pi^-$	$K_S^0\pi^0\pi^0$	$K_S^0\pi^0$	$K_S^0\omega$	$K_S^0\eta$	y_{CP}
Background	0.3	0.3	-	0.3	-	-	0.001
M_{BC} fit	0.4	0.1	2.4	0.4	0.1	1.4	0.001
U_{miss} fit ($Ke\nu$)	1.8	1.3	2.4	1.6	8.1	1.2	0.006
U_{miss} fit ($K\mu\nu$)	3.2	7.0	4.6	2.5	1.7	1.7	
Fake tag ($Ke\nu$)	0.2	1.4	0.9	1.2	3.1	0.4	0.002
Fake tag ($K\mu\nu$)	1.0	0.7	0.5	0.9	4.8	0.4	
CP -purity	-	-	0.4	-	0.2	0.2	0.001

examined by fitting to the M_{BC} versus U_{miss} two-dimensional plots. From this study, the fake tagged signal component is proved to be very small. The resulting difference on y_{CP} is 0.002 and assigned as a systematic uncertainty.

We study the CP -purities of ST modes by searching for same- CP DT signals in data. Assuming CP conservation in the charm sector, the same- CP process is prohibited, unless the studied CP modes are not pure or the initial C -odd $D^0\bar{D}^0$ system is diluted. The CP modes involving K_S^0 are not pure due to the existence of small CPV in $K^0 - \bar{K}^0$ mixing [6]. However, this small effect is negligible with our current sensitivity. Hence, $K_S^0\pi^0$ is assumed to be a clean CP mode, as its background level is very low. As a conservative treatment, we study DT yields of $(K_S^0\pi^0, K_S^0\pi^0)$ to verify its pure CP -odd eigenstate nature and the CP -odd environment of the $D^0\bar{D}^0$ pair. The observed numbers of this DT signals are quite small, and we estimate the dilution of the C -odd initial state to be less than 2% at 90% confidence level. This affects our measurement of y_{CP} by less than 0.001. The purity of the $K_S^0\pi^0$ mode is found to be larger than 99%. Due to the complexity of the involved non-resonant and resonant processes in $K_S^0\pi^0\pi^0$ and $K_S^0\omega$, the CP -purities of these tag modes could be contaminated. We take the mode K^+K^- as a clean CP -even tag to test $K_S^0\pi^0\pi^0$, and take $K_S^0\pi^0$ to test $K_S^0\omega$ and $K_S^0\eta$. The CP -purities of $K_S^0\pi^0\pi^0$, $K_S^0\omega$ and $K_S^0\eta$ are estimated to be larger than 89.4%, 93.3% and 93.9%, respectively. Based on the obtained CP purities, the corresponding maximum effect on the determined y_{CP} is assigned as systematic uncertainty.

Systematic uncertainties from different sources are assumed to be independent and are combined in quadrature to obtain the overall y_{CP} systematic uncertainties. The resultant total y_{CP} systematic uncertainties is 0.007.

4. Results

The branching ratios of $K^\mp e^\pm\nu$ and $K^\mp \mu^\pm\nu$ are summed to obtain $\mathcal{B}_{D_{CP^\mp}\rightarrow l} = \mathcal{B}_{D_{CP^\mp}\rightarrow Ke\nu} + \mathcal{B}_{D_{CP^\mp}\rightarrow K\mu\nu}$. To combine results from different CP modes, the standard weighted least-square method is utilized [6]. The weighted semileptonic branching fraction $\tilde{\mathcal{B}}_{D_{CP^\pm}\rightarrow l}$ is determined by minimizing

$$\chi^2 = \sum_{\alpha} \frac{\left(\tilde{\mathcal{B}}_{D_{CP^\pm}\rightarrow l} - \mathcal{B}_{D_{CP^\pm}\rightarrow l}^{\alpha}\right)^2}{\left(\sigma_{CP^\pm}^{\alpha}\right)^2}, \quad (10)$$

where α denotes different CP -tag modes and $\sigma_{CP^\pm}^{\alpha}$ is the statistical error of $\mathcal{B}_{D_{CP^\pm}\rightarrow l}^{\alpha}$ for the given tag mode. The branching fractions of $\mathcal{B}_{D_{CP^\pm}\rightarrow l}$ and the obtained $\tilde{\mathcal{B}}_{D_{CP^\pm}\rightarrow l}$ are listed in Table 5. Finally, y_{CP} is calculated using Eq. (3), with $\mathcal{B}_{D_{CP^\pm}\rightarrow l}$ replaced by $\tilde{\mathcal{B}}_{D_{CP^\pm}\rightarrow l}$. We obtain $y_{CP} = (-2.0 \pm 1.3 \pm 0.7)\%$, where the first uncertainty is statistical and the second is systematic.

5. Summary

Using quantum-correlated $D^0\bar{D}^0$ pairs produced at $\sqrt{s} = 3.773$ GeV, we employ a CP -tagging technique to obtain the y_{CP} parameter of $D^0 - \bar{D}^0$ oscillations. Under the assumption of no direct CPV in the D

Table 5: Values of branching ratio of $D_{CP\pm}\rightarrow l$ obtained from different tag modes and the combined branching ratio. The errors shown are statistical only.

Tag Mode	$\mathcal{B}_{D_{CP-}\rightarrow Ke\nu}$ (%)	$\mathcal{B}_{D_{CP-}\rightarrow K\mu\nu}$ (%)	$\mathcal{B}_{D_{CP-}\rightarrow l}$ (%)
K^+K^-	3.44 ± 0.12	3.33 ± 0.12	6.77 ± 0.17
$\pi^+\pi^-$	3.29 ± 0.18	3.35 ± 0.20	6.64 ± 0.27
$K_S^0\pi^0\pi^0$	3.40 ± 0.18	3.48 ± 0.18	6.89 ± 0.26
$\tilde{\mathcal{B}}_{D_{CP-}\rightarrow l}$	3.40 ± 0.09	3.37 ± 0.09	6.77 ± 0.12
Tag Mode	$\mathcal{B}_{D_{CP+}\rightarrow Ke\nu}$ (%)	$\mathcal{B}_{D_{CP+}\rightarrow K\mu\nu}$ (%)	$\mathcal{B}_{D_{CP+}\rightarrow l}$ (%)
$K_S^0\pi^0$	3.62 ± 0.10	3.33 ± 0.10	6.96 ± 0.15
$K_S^0\omega$	3.32 ± 0.21	3.81 ± 0.21	7.14 ± 0.30
$K_S^0\eta$	3.68 ± 0.26	3.84 ± 0.29	7.52 ± 0.40
$\tilde{\mathcal{B}}_{D_{CP+}\rightarrow l}$	3.58 ± 0.09	3.46 ± 0.09	7.04 ± 0.13

sector, we obtain $y_{CP} = (-2.0 \pm 1.3(\text{stat.}) \pm 0.7(\text{sys.}))\%$. This result is compatible with the previous measurements [18, 33, 34, 35] within about two standard deviations. However, the precision is still statistically limited and less precise than the current world average [6]. Future efforts using a global fit [36] may better exploit the BESIII data, leading to a more precise result.

6. Acknowledgments

The BESIII collaboration thanks the staff of BEPCII and the IHEP computing center for their strong support. This work is supported in part by National Key Basic Research Program of China under Contract No. 2015CB856700; Joint Funds of the National Natural Science Foundation of China under Contracts Nos. 11079008, 11179007, U1232201, U1332201; National Natural Science Foundation of China (NSFC) under Contracts Nos. 11125525, 11235011, 11275266, 11322544, 11335008, 11425524; the Chinese Academy of Sciences (CAS) Large-Scale Scientific Facility Program; CAS under Contracts Nos. KJCX2-YW-N29, KJCX2-YW-N45; 100 Talents Program of CAS; INPAC and Shanghai Key Laboratory for Particle Physics and Cosmology; German Research Foundation DFG under Contract No. Collaborative Research Center CRC-1044; Istituto Nazionale di Fisica Nucleare, Italy; Ministry of Development of Turkey under Contract No. DPT2006K-120470; Russian Foundation for Basic Research under Contract No. 14-07-91152; U. S. Department of Energy under Contracts Nos. DE-FG02-04ER41291, DE-FG02-05ER41374, DE-FG02-94ER40823, DESC0010118; U.S. National Science Foundation; University of Groningen (RuG) and the Helmholtzzentrum fuer Schwerionenforschung GmbH (GSI), Darmstadt; WCU Program of National Research Foundation of Korea under Contract No. R32-2008-000-10155-0.

References

- [1] S. Bianco, F. Fabbri, D. Benson, I. Bigi, Riv. Nuovo Cim. 26N7 (2003) 1.
- [2] Z.-Z. Xing, Phys. Rev. D 55 (1997) 196.
- [3] E. Boldt, D. O. Caldwell, Y. Pal, Phys. Rev. Lett. 1 (1958) 150.
- [4] H. Albrecht, et al. (ARGUS Collaboration), Phys. Lett. B 192 (1987) 245.
- [5] A. Abulencia, et al. (CDF Collaboration), Phys. Rev. Lett. 97 (2006) 242003.
- [6] K. Olive, et al. (Particle Data Group), Chin. Phys. C 38 (2014) 090001.
- [7] M. Staric, et al. (Belle Collaboration), Phys. Rev. Lett. 98 (2007) 211803.
- [8] B. Aubert, et al. (BaBar Collaboration), Phys. Rev. Lett. 98 (2007) 211802.
- [9] T. Aaltonen, et al. (CDF Collaboration), Phys. Rev. Lett. 100 (2008) 121802.
- [10] R. Aaij, et al. (LHCb Collaboration), Phys. Rev. Lett. 111 (2013) 251801.
- [11] T. A. Aaltonen, et al. (CDF Collaboration), Phys. Rev. Lett. 111 (2013) 231802.
- [12] B. Ko, et al. (Belle Collaboration), Phys. Rev. Lett. 112 (2014) 111801.
- [13] S. Bergmann, Y. Grossman, Z. Ligeti, Y. Nir, A. A. Petrov, Phys. Lett. B 486 (2000) 418.

- [14] N. Cabibbo, Phys. Rev. Lett. 10 (1963) 531.
- [15] M. Kobayashi, T. Maskawa, Prog. Theor. Phys. 49 (1973) 652.
- [16] S. L. Glashow, J. Illiopoulos, L. Maiani, Phys. Rev. D 2 (1970) 1285.
- [17] T. Browder, S. Pakvasa, Phys. Lett. B 383 (1996) 475.
- [18] Y. Amhis, et al. (Heavy Flavor Averaging Group) (2014). [arXiv:1412.7515](https://arxiv.org/abs/1412.7515), and online update at <http://www.slac.stanford.edu/xorg/hfag/>.
- [19] M. Gronau, Y. Grossman, J. L. Rosner, Phys. Lett. B 508 (2001) 37.
- [20] D. Atwood, A. A. Petrov, Phys. Rev. D 71 (2005) 054032.
- [21] X.-D. Cheng, et al., Phys. Rev. D 75 (2007) 094019.
- [22] D. Asner, W. Sun, Phys. Rev. D 73 (2006) 034024.
- [23] M. Ablikim, et al. (BESIII Collaboration), Chin. Phys. C 37 (2013) 123001.
- [24] M. Ablikim, et al. (BESIII Collaboration), Nucl. Instrum. Meth. A 614 (2010) 345.
- [25] C. Zhang, Sci. China G 53 (2010) 2084.
- [26] S. Agostinelli, et al. (GENAT4 Collaboration), Nucl. Instrum. Meth. A 506 (2003) 250.
- [27] S. Jadach, et al., Phys. Rev. D 63 (2001) 113009.
- [28] D. J. Lange, Nucl. Instrum. Meth. A 462 (2001) 152.
- [29] R. G. Ping, et al., Chin. Phys. C 32 (2008) 599.
- [30] J. C. Chen, et al., Phys. Rev. D 62 (2000) 034003.
- [31] E. Richter-Was, Phys. Lett. B 303 (1993) 163.
- [32] H. Albrecht, et al. (ARGUS Collaboration), Phys. Lett. B 241 (1990) 278.
- [33] J. Lees, et al. (BaBar Collaboration), Phys. Rev. D 87 (2013) 012004.
- [34] M. Starič (BaBar Collaboration) (2012). [arXiv:1212.3478](https://arxiv.org/abs/1212.3478).
- [35] R. Aaij, et al. (LHCb Collaboration), Phys. Rev. Lett. 112 (2014) 041801.
- [36] Y. Guan, X.-R. Lu, Y. Zheng, Y.-Z. Zhu, Chin. Phys. C 37 (2013) 106201.